Molecular Crystals and Liquid Crystals

Taylor & Francis
Taylor & Francis Group

ISSN: 1542-1406 (Print) 1563-5287 (Online) Journal homepage: https://www.tandfonline.com/loi/gmcl20

Improvement of MgO Characteristics Using RF-Plasma Treatment in AC Plasma Display Panel

Choon-Sang Park & Heung-Sik Tae

To cite this article: Choon-Sang Park & Heung-Sik Tae (2010) Improvement of MgO Characteristics Using RF-Plasma Treatment in AC Plasma Display Panel, Molecular Crystals and Liquid Crystals, 531:1, 73/[373]-81/[381], DOI: 10.1080/15421406.2010.499331

To link to this article: https://doi.org/10.1080/15421406.2010.499331

Published online: 14 Nov 2010.

Submit your article to this journal

Article views: 46

View related articles

Full Terms & Conditions of access and use can be found at
https://www.tandfonline.com/action/journalInformation?journalCode=gmcl20

Mol. Cryst. Liq. Cryst., Vol. 531: pp. 73/[373]–81/[381], 2010
Copyright © Taylor & Francis Group, LLC
ISSN: 1542-1406 print/1563-5287 online
DOI: 10.1080/15421406.2010.499331

Taylor & Francis
Taylor & Francis Group

Improvement of MgO Characteristics Using RF-Plasma Treatment in AC Plasma Display Panel

CHOON-SANG PARK AND HEUNG-SIK TAE

School of Electrical Engineering and Computer Science, Kyungpook National University, Daegu, Korea

The characteristics of the MgO layer are known to be an important parameter that affects the discharge characteristics in an ac-PDP. In this paper, to improve the MgO characteristics of 50-in. full-HD ac-PDP with He (35%) – Xe (11%) contents, RF-plasma treatments on the MgO layer are examined under various gases for plasma treatment. The resultant changes in the MgO characteristics, including the morphology, roughness, secondary electron coefficient, and firing voltage, were examined in comparison with both cases with and without plasma treatment on the MgO layer. It is concluded that the Ar and Ar > O_2 plasma treatments can enhance the MgO characteristics, such as the roughness, secondary electron coefficient, and firing voltage.

Keywords AFM; firing voltage; 50-in. full-HD AC-PDP module; MgO; morphology; plasma treatment; roughness; secondary electron coefficient; SEM; Vt closed curve

1. Introduction

The MgO layers have been used as a protective layer in ac-PDPs due to their high stability against ion bombardment, low optical loss, high thermal stability, and good electrical insulating properties. Moreover, the MgO layers play a significant role in reducing the discharge voltage of ac-PDPs due to their high secondary electron emission capability and thus, various attempts to improve the characteristics of these layers have been reported [1–11].

In this paper, the MgO surface modification using the RF-plasma treatment with variable plasma gas compositions were adopted to improve the MgO surface characteristics. In particular, the RF-plasma treatment used the three kinds of plasma gas compositions such as $O_2 > Ar$ (O_2: 201 sccm, Ar: 22 sccm), Ar (240 sccm), and $Ar > O_2$ (Ar: 189 sccm, O_2: 21 sccm), in order to investigate which gas in RF-plasma treatment can contribute to modifying the MgO surface for the better discharge characteristics of ac-PDP. The resultant changes in the MgO and discharge

Address correspondence to Prof. Heung-Sik Tae, School of Electrical Engineering and Computer Science, Kyungpook National University, Sangyuk-dong, Buk-gu, Daegu 702-701, Korea (ROK). Tel.: (+82)53-950-6563; Fax: (+82)53-950-5505; E-mail: hstae@ee.knu.ac.kr

characteristics, such as the morphology, roughness, secondary electron coefficient, and firing voltage were examined in comparison with the non-plasma treatment on MgO layer in the 50-in. full-HD ac-PDP with He (35%) – Xe (11%) contents.

2. Experimental Setup

Figure 1 shows the optical-measurement systems and 50-in. full-HD ac-PDP module with three electrodes used in the experiments, where X is the sustain electrode, Y the scan electrode, and A the address electrode. A pattern generator, signal generator, and photo-sensor amplifier (Hamamatsu, C6386) were used to measure the IR emission and Vt closed curve, respectively.

Figure 2 shows the single pixel structure of the 50-in. full-HD AC-PDP panel employed in this research. The detailed panel specifications are listed in Table 1.

Figure 3 shows a schematic diagram of the RF-plasma equipment used for the plasma treatment system. Tables 2 and 3 show the specifications of the RF-plasma

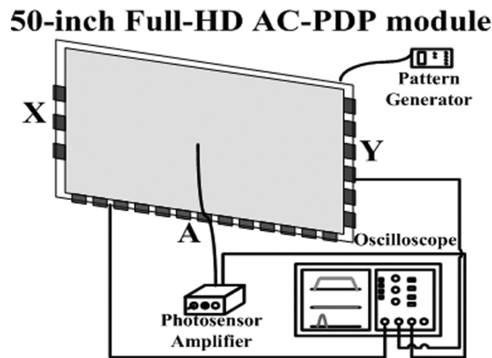

Figure 1. Schematic diagram of experimental setup employed in this research.

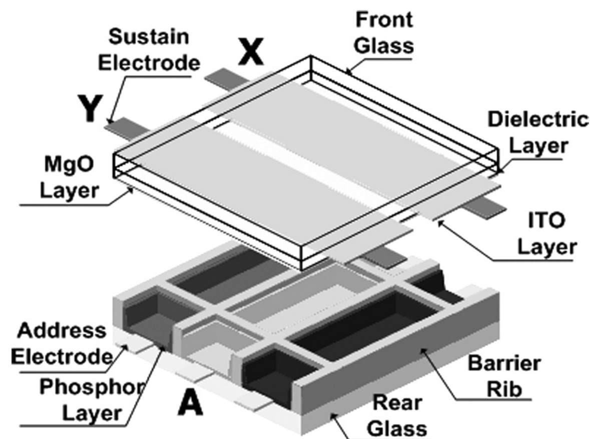

Figure 2. Schematic diagram of single pixel structure in 50-inch full-HD AC-PDP.

Table 1. Specifications of 50-inch full-HD AC-PDP used in this study

Front panel		Rear panel	
ITO width	210 μm	Barrier rib width	50 μm
ITO gap	70 μm	Barrier rib height	120 μm
Bus width	70 μm	Address width	85 μm
Pixel pitch		$576 \times 576\,\mu m^2$	
Gas chemistry		Ne-Xe (11%)-He (35%)	
Gas pressure		430 Torr	
Barrier rib type		Closed rib	

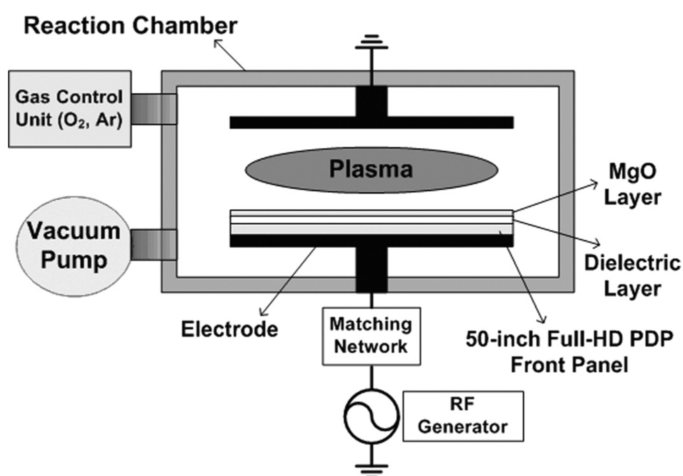

Figure 3. Schematic diagram of RF plasma equipment used for plasma treatment system.

treatment condition and variable plasma treatment gas compositions employed in this research, which were exactly the same, except for the plasma treatment gas composition. The RF (13.56 MHz) input power and the process time for plasma treatment were 4 kW and 30 minutes, respectively.

Table 2. Specifications of plasma treatment condition employed in this research

	Plasma treatment condition (Set-up)
Plasma type	RIE (Reactive ion etching) plasma generator
Vacuum pump	Dry pump (base pressure:4.3 mtorr)
RF (13.56 MHz) input power	4 kW
Operating pressure	100 mtorr
Process time	30 minutes

Table 3. Specifications of variable plasma treatment gas compositions employed in this research

	Plasma treatment gas compositions
Ref. (non-plasma treatment)	Non plasma treatment
$O_2 > Ar$ Plasma treatment	O_2 (201 sccm) + Ar (22 sccm)
Ar Plasma treatment	Ar (240 sccm)
$Ar > O_2$ Plasma treatment	Ar (189 sccm) + O_2 (21 sccm)

3. Experimental Observation on MgO Characteristics Using RF-Plasma Treatments Under Various Gases for Plasma Treatment

3.1. *Monitoring of Morphology and Roughness of MgO Layer*

Figure 4 shows the changes in the plane-SEM image of the MgO surfaces in 50-in. test panels prepared using the RF-plasma treatment on the MgO layer with variable

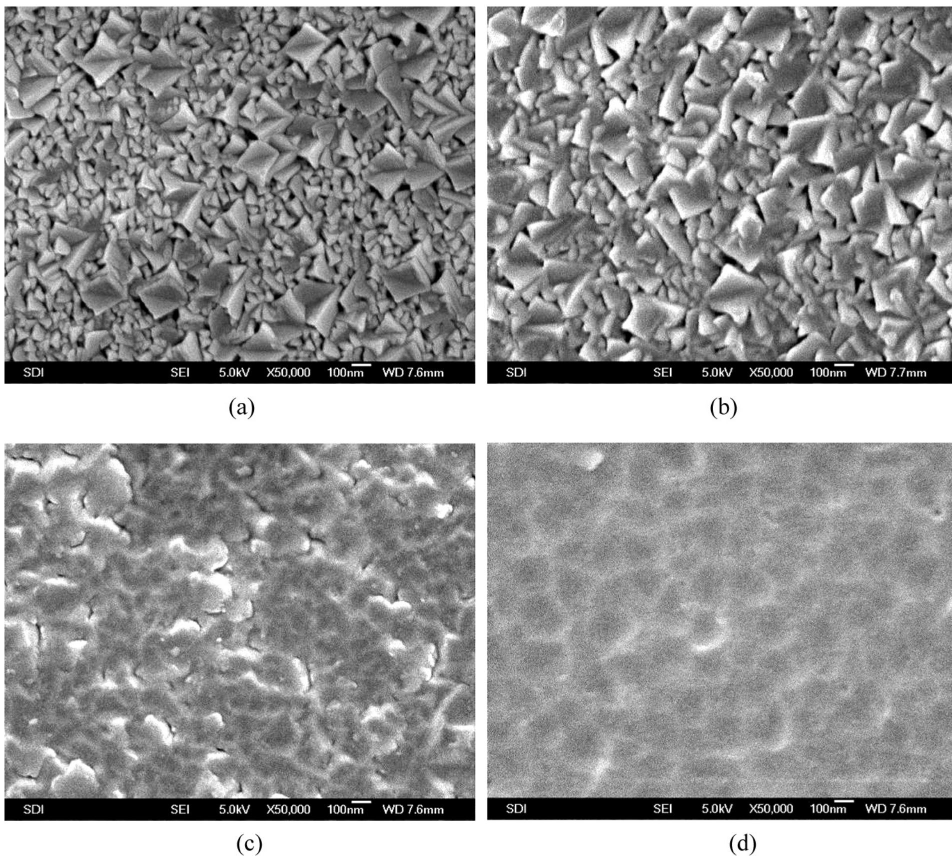

Figure 4. Comparison of plane-SEM image of MgO surface measured from 50-inch full-HD panels using RF-plasma treatment on MgO layer with variable gas compositions. (a) Ref. panel (non-plasma treatment), (b) $O_2 > Ar$ plasma treatment panel, (c) Ar plasma treatment panel, and (d) $Ar > O_2$ plasma treatment panel.

plasma gas compositions: (a) non-plasma treatment, (b) $O_2 > Ar$, (c) Ar, and (d) $Ar > O_2$ plasma treatments. As shown in Figure 4, in the case of $O_2 > Ar$ plasma treatment, the surface morphology of the MgO layer were almost same in comparison with the non-plasma treatment (Ref. panel). However, in the cases of Ar and $Ar > O_2$ plasma treatments, the surface morphology of the MgO layer were remarkably changed in comparison with the non-plasma treatment. The pyramidal morphology of grains on the MgO surfaces in the cases of Ar and $Ar > O_2$ plasma treatments were eliminated, as shown by the SEM image in Figure 4, and this elimination of grains on the MgO surface was mainly due to the physical sputtering caused by the ion bombardment during the Ar and $Ar > O_2$ plasma treatments.

Figure 5 and Table 4 show the changes in the 3-dimensional AFM images and roughness of the MgO surface in 50-in. test panels prepared using the RF-plasma treatment on the MgO layer with variable plasma gas compositions. As shown in Figures 5(a) and (b), and Table 4, in the case of $O_2 > Ar$ plasma treatment, the roughness of the MgO layer were slightly reduced in comparison with the non-plasma treatment (Ref. panel). However, as shown in Figures 5(c) and (d), and Table 4, in the cases of Ar and $Ar > O_2$ plasma treatments, the roughness of the MgO layer were remarkably reduced in comparison with the non-plasma treatment.

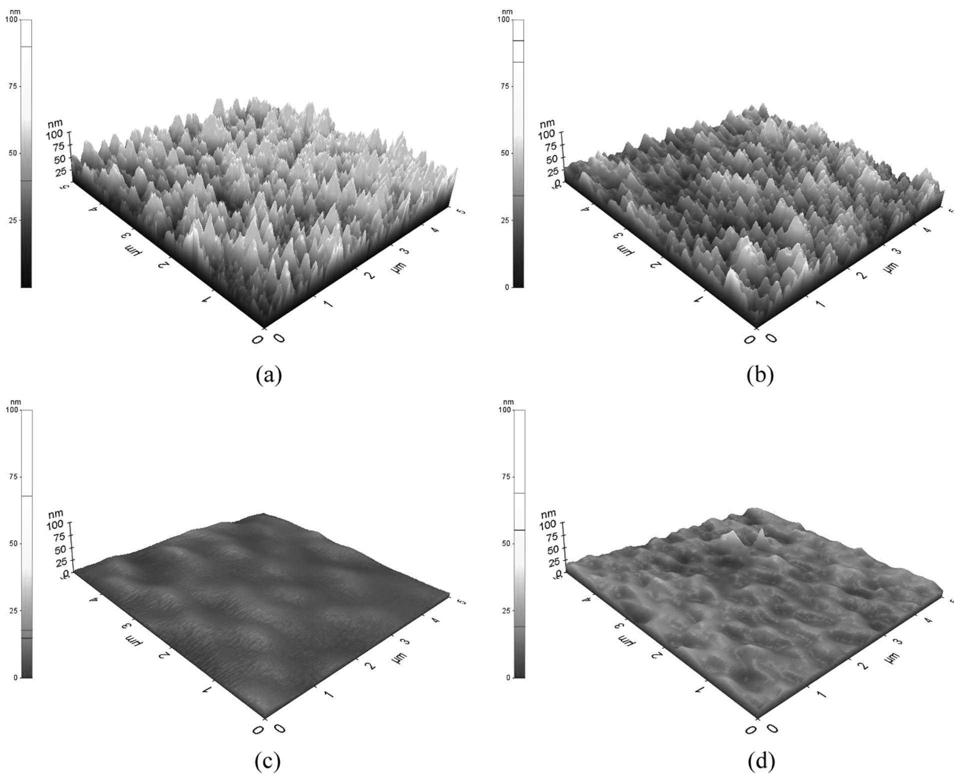

Figure 5. Comparison of 3-D AFM images of MgO surface measured from 50-inch full-HD panels using RF-plasma treatment on MgO layer with variable gas compositions. (a) Ref. panel (non-plasma treatment), (b) $O_2 > Ar$ plasma treatment panel, (c) Ar plasma treatment panel, and (d) $Ar > O_2$ plasma treatment panel.

Table 4. Comparison of roughness of MgO surface measured from 50-inch full-HD panels using RF-plasma treatment on MgO layer with variable gas compositions

	Roughness [Rrms, Å]
Ref. (non-plasma treatment)	136.69
$O_2 > Ar$ Plasma treatment	116.22
Ar Plasma treatment	22.39
$Ar > O_2$ Plasma treatment	46.29

3.2. *Monitoring of Secondary Electron Emission of MgO Layer*

Figure 6 shows the changes in the secondary electron coefficients (γ) for the MgO layers measured from 50-in. test panels prepared using the RF-plasma treatment on the MgO layer with variable gas compositions. The secondary electron emission for the MgO layer was measured using the γ-FIB (Focused Ion Beam) system. The γ-FIB system measured the intensity of the electrons emitted from the MgO layer when the MgO surface was struck by the Ne^+ ions focused to a diameter of 80 μm by means of a single Einzel lens with ion acceleration energy ranging from 80 to 200 V [12]. As shown in Figure 6, in the case of Ar and $Ar > O_2$ plasma treatments, the secondary electron coefficients for the MgO layer were higher than that for the MgO layer in the non-plasma treatment and $O_2 > Ar$ plasma treatment, indicating that the MgO surface state was enhanced by means of the physical sputtering caused by the Ar or $Ar > O_2$ RF-plasma treatment. However, the other research result has been reported that the oxygen RF-plasma treatment contributes to improving the secondary electron emission of the MgO layer [9,10]. The oxygen vacancy of the initial MgO layer can affect which RF-plasma treatment, that is, Ar or O_2, contributes to improving the secondary electron emission of the MgO layer.

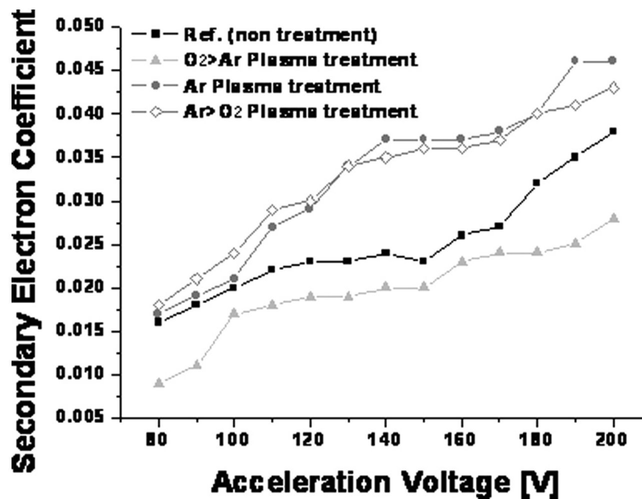

Figure 6. Comparison of secondary electron coefficients measured from 50-inch full-HD panels using RF-plasma treatment on MgO layer with variable gas compositions.

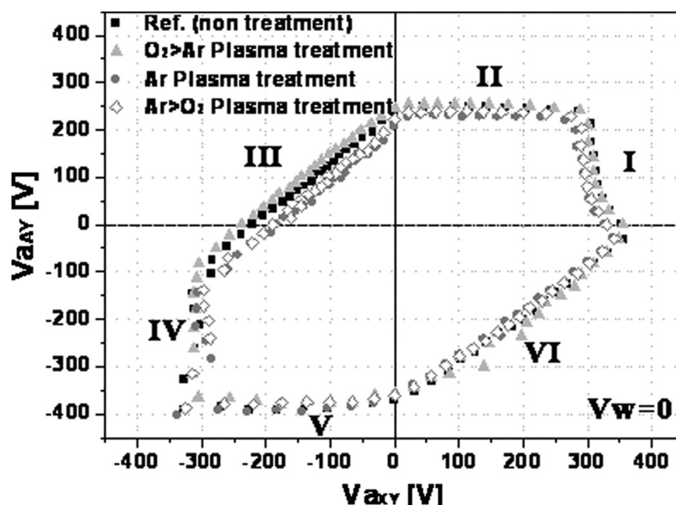

Figure 7. Comparison of Vt closed curves between 50-inch full-HD panels using RF-plasma treatment on MgO layer with variable gas compositions without initial wall charges where I: V_{tXY} (= Discharge start threshold cell voltage between X and Y), II: V_{tAY} (= Discharge start threshold cell voltage between A and Y), III: V_{tAX} (= Discharge start threshold cell voltage between A and X), IV: V_{tYX} (= Discharge start threshold cell voltage between Y and X), V: V_{tYA} (= Discharge start threshold cell voltage between Y and A), and VI: V_{tXA} (= Discharge ischarge start threshold cell voltage between X and A).

4. Analysis on MgO Surface Change and Related Firing Voltages Using Vt Closed Curve Technique

Figure 7 shows the changes in the Vt closed curves under no initial wall charges in 50-in. test panels prepared using the RF-plasma treatment on the MgO layer with variable plasma gas compositions: non-plasma treatment, $O_2 > Ar$, Ar, and $Ar > O_2$ plasma treatments. As shown in Figure 7, in the cases of Ar and $Ar > O_2$ plasma treatments, the firing voltages for I(X-Y), II(A-Y), III(A-X), and IV(Y-X), i.e., the firing voltages under MgO cathode conditions, were remarkably reduced,

Table 5. Firing voltages measured from 50-inch full-HD panels using RF-plasma treatment on MgO layer with variable gas compositions

		Firing voltage			
Region		Ref.	$O_2 > Ar$	Ar	$Ar > O_2$
MgO Cathode	I	320.06 V	320.00 V	294.42 V	312.54 V
	II	250.71 V	259.67 V	238.89 V	249.83 V
	III	223.86 V	243.45 V	211.08 V	224.82 V
	IV	317.90 V	313.06 V	286.65 V	278.17 V
Phosphor Cathode	V	393.19 V	395.07 V	393.87 V	380.99 V
	VI	391.29 V	410.54 V	383.29 V	390.35 V

whereas the firing voltages for V(Y-A) and VI(X-A), i.e., the firing voltages under phosphor cathode conditions, were almost same. In the cases of Ar and Ar > O_2 plasma treatments, the firing voltages under the MgO cathode conditions were remarkably reduced due to the increase in the secondary electron coefficient for the MgO layer. Table 5 shows the variations in the firing voltages measured under the MgO and phosphor cathode conditions for the 50-in. test panels prepared using the RF-plasma treatment on the MgO layer with variable plasma gas compositions. These experimental results confirm that the Ar and Ar > O_2 plasma treatments can modify the MgO surface state, thereby contributing to improving the discharge characteristics of the PDP-TV.

5. Conclusion

In this paper, the RF-plasma treatment to enhance characteristics of the MgO layer was adopted, and the resultant changes in the MgO characteristics, such as roughness, secondary electron coefficient, and firing voltage were examined in comparison with both cases with and without plasma treatment on MgO layer in the 50-in. full-HD ac-PDP with He (35%) – Xe (11%) contents. It is concluded that the Ar and Ar > O_2 plasma treatments can enhance the MgO characteristics, such as the roughness, secondary electron coefficient, and firing voltage. Thus, it is expected that these experimental results can contribute to improve the MgO and the discharge characteristics of the PDP-TV.

Acknowledgments

This work was supported in part by the IT R&D program of MKE/KEIT and in part by the Brain Korea 21 (BK21).

References

[1] Lee, G. S., Kim, K. B., Kim, J. J., & Sohn, S. H. (2009). *J. Phys. D: Appl. Phys.*, *42*(105402), 1–5.
[2] Seo, G.-W., Kim, J.-B., Park, S.-T., Kim, K.-T., Seo, Y.-W., Kim, S.-G., Kim, D.-Y., Seo, J.-M., Park, D.-H., Park, M.-S., & Ryu, B.-G. (2006). *SID '06*, *37*, 547–549.
[3] Kajiyama, H., Tanno, H., Shinoda, T., Fukasawa, T., Ramasamy, R., Shanmugavelayutham, G., & Yasuda, T. (2007). *SID '07*, *38*, 1321–1324.
[4] Park, C.-S., Tae, H.-S., Kwon, Y.-K., & Heo, E. G. (2008). *IEEE Trans. Plasma Science*, *36*(4), 1925–1929.
[5] Park, C.-S., Tae, H.-S., Kwon, Y.-K., & Heo, E. G. (2009). *Mol. Cryst. Liq. Cryst.*, *499*, 224–233.
[6] Lee, S., & Ito, T. (2005). *Materials Research Bulletin*, *40*(6), 951–961.
[7] Moon, S. H., Heo, T. W., Park, S. Y., Kim, J. H., & Kim, H. J. (2007). *J. Electrochemical Soc.*, *154*(12), J408–J412.
[8] Park, C.-S., Tae, H.-S., Kwon, Y.-K., & Heo, E. G. (2007). *IEEE Trans. Electron Devices*, *54*(6), 1315–1320.
[9] Jeong, W. H., Jeong, K. W., Lim, Y. C., Oh, H. J., Park, C. W., Choi, E. H., Seo, Y. H., Kim, Y. K., & Kang, S. O. (2006). *IDW '06*, *13*, 1145–1148.

[10] Son, C. G., Lee, H. J., Han, Y. G., Jeong, S. H., Yoo, N. L., Lee, S. B., Lim, J. E., Lee, J. H., Ko, B. D., Jeoung, J. M., Moon, M. W., Oh, P. Y., Juung, J. C., Park, W. B., & Choi, E. H. (2005). *IDW '05*, *12*, 1519–1522.
[11] Lee, S. H., Rhee, B. J., Joo, M. H., Kang, J., Chung, J. S., & Park, M.-H. (2003). *Surface and Coating Technology*, *171*, 247–251.
[12] Choi, E.-H., Oh, H.-J., Kim, Y.-G., Ko, J.-J., Lim, J.-Y., Kim, J.-G., Kim, D.-I., Cho, G., & Kang, S.-O. (1998). *Jpn. J. Appl. Phys.*, *37*(12B), 7015–7018.